

# On allowing for transient variation in end-member $\delta^{13}\text{C}$ values in partitioning soil C fluxes from net ecosystem respiration

Christopher S. McCloskey<sup>1,2</sup>  | Wilfred Otten<sup>1</sup>  | Eric Paterson<sup>2</sup>  |  
Guy J. D. Kirk<sup>1</sup> 

<sup>1</sup>School of Water, Energy and Environment, Cranfield University, Bedford, UK

<sup>2</sup>The James Hutton Institute, Aberdeen, UK

## Correspondence

Guy J. D. Kirk, School of Water, Energy and Environment, Cranfield University, Cranfield, Bedford MK43 0AL, UK.  
Email: g.kirk@Cranfield.ac.uk

## Funding information

Natural Environment Research Council, Grant/Award Number: NE-M009106-1; Royal Society, Grant/Award Number: WL080021/Kirk; Rural and Environment Science and Analytical Services Division; Biotechnology and Biological Sciences Research Council

## Abstract

The use of stable isotope analysis to resolve ecosystem respiration into its plant and soil components rests on how well the end-member isotope signatures ( $\delta^{13}\text{C}$ ) are characterised. In general, it is assumed that end-member values are constant over time. However, there are necessarily diurnal and other transient variations in end-members with environmental conditions. We analyse diurnal and seasonal patterns of ecosystem respiration and its  $\delta^{13}\text{C}$  in a  $\text{C}_4$  grass growing in a  $\text{C}_3$  soil using fixed and diurnally varying plant and soil  $\delta^{13}\text{C}$  end-members. We measure the end-members independently, and we assess the effects of expected variation in values. We show that variation in end-members within realistic ranges, particularly diurnal changes in the plant end-member, can cause partitioning errors of 40% during periods of high plant growth. The effect depends on how close the end-member is to the measured net respiration  $\delta^{13}\text{C}$ , that is, the proportion of the respiration due to that end-member. We show light-driven variation in plant end-members can cause substantial distortion of partitioned soil organic matter (SOM) flux patterns on a diurnal scale and cause underestimation of daily to annual SOM turnover of approximately 25%. We conclude that, while it is not practicable to independently measure the full temporal variation in end-member values over a growing season, this error may be adjusted for by using a diurnally varying  $\delta^{13}\text{C}_{\text{plant}}$ .

## Highlights

- End-member  $\delta^{13}\text{C}$  values used to partition ecosystem respiration vary diurnally and seasonally
- Patterns of ecosystem respiration and its  $\delta^{13}\text{C}$  in a  $\text{C}_4$  grass growing in a  $\text{C}_3$  soil were analysed.

This is an open access article under the terms of the Creative Commons Attribution License, which permits use, distribution and reproduction in any medium, provided the original work is properly cited.

© 2021 The Authors. *European Journal of Soil Science* published by John Wiley & Sons Ltd on behalf of British Society of Soil Science.

- Ignoring temporal changes in end-member  $\delta^{13}\text{C}$  values can cause large errors in partitioning
- Long-term data sets with sufficient temporal resolution can be used to correct for this

#### KEYWORDS

$\text{C}_3$  and  $\text{C}_4$  photosynthesis, ecosystem respiration, isotopic flux partitioning, natural abundance, rhizosphere priming effect, soil carbon

## 1 | INTRODUCTION

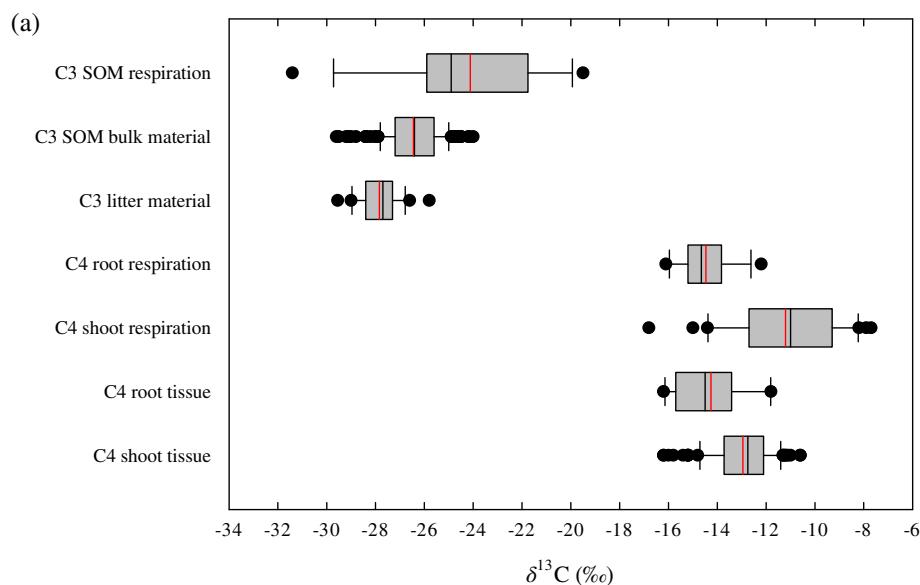
The effects of plant roots and rhizodeposition on soil organic matter (SOM) turnover remain among the most poorly understood aspects of the terrestrial carbon (C) cycle (Hartmann et al., 2020). A major factor is the difficulty of separating C fluxes from plants and rhizodeposition from those from SOM turnover. One way of doing this is to exploit differences in the C isotope composition of plants and SOM (Brüggemann et al., 2011; Paterson et al., 2009; Werth & Kuzyakov, 2010). Isotopic fractionations occur in most biochemical and biophysical processes, favouring either  $^{12}\text{C}$  or  $^{13}\text{C}$ . Hence, SOM is typically enriched in  $^{13}\text{C}$  compared to the plants from which it was derived by 2‰–4‰ (Bowling et al., 2008). The  $\delta^{13}\text{C}$  of the net plant and soil flux will lie between the plant and SOM ‘end-member’ values (i.e., the values for the plants and soil separately), and so can be used to partition fluxes with a mass balance mixing model. Differences of 2‰–4‰ are close to the quantitation limits of currently available analytical methods. But larger differences can be created, either by labelling plants with  $\text{CO}_2$  enriched or depleted in  $^{13}\text{C}$ , or, more practicably under field conditions, by exploiting the large  $\delta^{13}\text{C}$  difference between  $\text{C}_3$  and  $\text{C}_4$  photosynthetic pathways, which is typically 10‰–20‰ (Balesdent et al., 1987; Farquhar et al., 1989). This may be done by growing a  $\text{C}_4$  plant in a soil that has previously only hosted  $\text{C}_3$  plants, or vice-versa (Rochette & Flanagan, 1997; Wang et al., 2016; Xiao et al., 2015), or with natural  $\delta^{13}\text{C}$  gradients across transects of  $\text{C}_3$ – $\text{C}_4$  vegetation (Millard et al., 2008). In all cases, however, reliable partitioning of plant and SOM respiration fluxes depends on how well the  $\delta^{13}\text{C}$  C end-members are characterised. This paper is about how best to do this and how to allow for transient variation in end-members which as yet has been largely overlooked in the flux partitioning literature (Lee et al., 2020; Ogle & Pendall, 2015).

Wide variation in  $\delta^{13}\text{C}$  values are reported for  $\text{C}_4$  plants and  $\text{C}_3$  soils (Figure 1). The largest variation is between photosynthetic pathways, but there is substantial variation within  $\text{C}_4$  plants (–16‰ to –8‰) and  $\text{C}_3$

soils (–30‰ to –20‰). Some of this is due to differences in measurement methods, such as with instrument calibration, as well as inherent differences within plant species and soil types. However a large part is due to transient variation driven by environmental factors. Water stress can cause large  $\delta^{13}\text{C}$  shifts in  $\text{C}_3$  species, but this effect is small in  $\text{C}_4$  plants, typically <1‰, owing to their greater water use efficiency (Cernusak et al., 2013; Ghannoum et al., 2002). Of particular importance is climatic, seasonal and diurnal variation in light intensity; this causes differences in both  $\text{C}_3$  and  $\text{C}_4$  plant  $\delta^{13}\text{C}$  of 1‰–8‰ (Cernusak et al., 2013; Cornwell et al., 2018; Ghashghaie & Badeck, 2014). Leaf respiration immediately after a period of illumination is  $^{13}\text{C}$ -enriched, whereas it is progressively  $^{13}\text{C}$ -depleted during darkness. In  $\text{C}_3$  grasses, Barbour et al. (2005) observed a decrease in  $\delta^{13}\text{C}$  of approximately 5‰ over 6 h of darkness, with the change almost entirely taking place in the first 2 h, and Tcherkez et al. (2003) found a decrease of approximately 10‰ over 5 days in a  $\text{C}_3$  forb. There have been fewer studies in  $\text{C}_4$  species, but Sun et al. (2010) and Zhong et al. (2017) found decreases from 1‰ to 4‰ (mostly 2‰–4‰) over 6 h of dark in  $\text{C}_4$  grasses. The daytime  $^{13}\text{C}$  enrichment is linked to differences in C substrate availability and metabolite partitioning during photosynthesis (Ghashghaie & Badeck, 2014; Sun et al., 2010; Zhong et al., 2017).

Soil isotopic composition is less affected by short-term variation in environmental conditions (Buchman et al., 1997; Scartazza et al., 2004), although environmentally driven variability in microbial fractionation has been observed (Lerch et al., 2011). There is variation in the  $\delta^{13}\text{C}$  of SOM pools and respiration with soil depth, in part due to differences between litter and SOM (Figure 1) but also due to biophysical processes (Boström et al., 2007; Nickerson & Risk, 2009; Trudell et al., 2004). Inputs of plant residues and root exudates vary with depth and follow seasonal patterns, and differences in the rates of decomposition of different inputs add to temporal variation in the  $\delta^{13}\text{C}$  of cycling SOM pools (Werth & Kuzyakov, 2010). Hence, the  $\delta^{13}\text{C}$  of SOM respiration may differ from that of the bulk SOM and may also vary

**FIGURE 1** (a) Range of reported  $\delta^{13}\text{C}$  values for  $\text{C}_3$  soil and  $\text{C}_4$  plant pools and respiration fluxes. Boxes indicate 25th, 50th and 75th percentiles; whiskers 10th and 90th percentiles; red lines means. (b) Numbers of reported values ( $n$ ; NB in studies with treatment replicates  $n = 1$ ) and references. Studies were excluded where plants were not grown under atmospheric  $\delta^{13}\text{C}$  conditions, for soil organic matter (SOM) respiration where roots were not excluded, and where only relative fractionation of  $^{13}\text{C}$  (rather than  $\delta^{13}\text{C}$ ) was given



Pool or flux	<i>n</i>	Reference
C <sub>3</sub> SOM respiration	13	Boström et al. (2007); Pausch and Kuzyakov (2012); Snell et al. (2014); Werth and Kuzyakov (2006)
C <sub>3</sub> SOM bulk material	171	Barbour et al. (2005); Boström et al. (2007); Bowling et al. (2002, 2003); Fessenden and Ehleringer (2003); Flanagan et al. (1996); Fu and Cheng (2002); Hemming et al. (2005); Hobbie et al. (1999, 2001); Kohzu et al. (1999); Kramer and Gleixner (2006); Pausch and Kuzyakov (2012); Scartazza et al. (2004); Trudell et al. (2004); Werth and Kuzyakov (2008, 2009)
C <sub>3</sub> litter	28	Barbour et al. (2005); Boström et al. (2007); Bowling et al. (2002); Fessenden and Ehleringer (2003); Hobbie et al. (2001); Kohzu et al. (1999); Scartazza et al. (2004)
C <sub>4</sub> root respiration	16	Lloyd et al. (2016); Millard et al. (2008); Pausch and Kuzyakov (2012); Werth and Kuzyakov (2006)
C <sub>4</sub> shoot respiration	30	Sun et al. (2010); Zhong et al. (2017)
C <sub>4</sub> root tissue	15	Rochette and Flanagan (1997); Wedinet al. (1995); Werth and Kuzyakov (2006, 2008, 2009); Zhu and Cheng (2011)
C <sub>4</sub> shoot tissue	102	Ghannoum et al. (2002); Hattersley (1982); Weiguo et al. (2005); Rochette and Flanagan (1997); Sun et al. (2010); von Caemmerer et al. (2014); G. Wang et al. (2005); Wedin et al. (1995); Werth and Kuzyakov (2006, 2008, 2009); Zhu and Cheng (2011)

over a season. Few studies have measured the  $\delta^{13}\text{C}$  of both bulk root-free soil and its respiration, and those that have report contrasting differences (Boström et al., 2007; Pausch & Kuzyakov, 2012). Fractionation between microbial biomass (itself more  $^{13}\text{C}$  enriched than SOM) and microbial respiration is highly variable, ranging from +4.3‰ to −3.2‰ (Werth & Kuzyakov, 2010). Further, in a  $\text{C}_3$  to  $\text{C}_4$  vegetation change, the  $\text{C}_4$  inputs will gradually become incorporated into the SOM, potentially providing a means of separating SOM pools but also complicating end-member evaluations.

What does this mean for partitioning soil C fluxes and whether or not to allow for transient variation in end-member  $\delta^{13}\text{C}$  values? Although temporal variation in end-members has been allowed for in partitioning

photosynthetic and respiration fluxes in net  $\text{CO}_2$  exchange (Fassbinder et al., 2012; Wehr & Saleska, 2015), as far as we are aware, the effects have not been assessed for partitioning plant and soil respiration fluxes. In principle, partitioning errors on diurnal and other short time-scales can affect both the inferred short-term variation in SOM fluxes and longer-term seasonal and annual dynamics and resulting conclusions about plant and soil processes. In this paper, we explore this with a data set of diurnal and seasonal patterns of C fluxes and  $\delta^{13}\text{C}$  in a  $\text{C}_4$  plant– $\text{C}_3$  soil field system. We focus on diurnal variation in the plant end-member given its inevitability and known importance. We use as baseline end-members the  $\delta^{13}\text{C}$  of plant and soil dry matter sampled from the field, which integrate short-term variations (Cernusak et al.,

2013). We assess the sensitivity of partitioning to the plant and soil end-members within realistic ranges, and the effect of diurnal changes in the plant end-member.

## 2 | MATERIALS AND METHODS

### 2.1 | Respiration measurements and partitioning

Measurements were made using the field laboratory system described in McCloskey et al. (2020). Briefly, the system contains 24 0.8-m diameter, 1-m deep soil monoliths in lysimeters, connected to automated gas-flux chambers and instruments for gas and stable isotope measurements. The data used in this analysis are for 12 lysimeters of a poorly drained, seasonally waterlogged loamy soil over clay, formerly under old C<sub>3</sub> pasture at Temple Balsall, Warwickshire and sampled as undisturbed, naturally structured monoliths. The soil was sown with C<sub>4</sub> buffalo grass (*Bouteloua dactyloides*) in January 2018 and then maintained under ambient field conditions, with periodic clipping to maintain an approximately 10-cm high sward.

During a plant and soil respiration measurement, an opaque lysimeter chamber is closed with an opaque lid and air in the headspace is circulated via a sampling loop to a gas analyser (Picarro G2201-*i* cavity ring-down spectroscopy instrument, calibrated against a Thermo Finnigan Delta<sup>Plus</sup> XP isotope ratio mass spectrometer as described in McCloskey et al., 2020) for near continuous measurement of the headspace CO<sub>2</sub> concentration and its  $\delta^{13}\text{C}$ . The total sampling and measurement interval is approximately 20 min, allowing three measurements in each of the 12 lysimeters over 24 h. The combined plant and soil respiration flux ( $F_R$ ) is found from the rate of change in headspace concentration after a period of equilibration, and its isotope ratio ( $\delta^{13}\text{C}_R$ ) is found from plots of  $\delta^{13}\text{C}$  versus the inverse of the CO<sub>2</sub> concentration according to the Keeling plot method (McCloskey et al., 2020). The flux is then partitioned between C<sub>3</sub> SOM and C<sub>4</sub> plant sources as follows. By definition

$$F_R = F_{\text{plant}} + F_{\text{SOM}} \quad (1)$$

$$F_{\text{plant}} = f_{\text{plant}} F_R \quad (2)$$

$$F_{\text{SOM}} = f_{\text{SOM}} F_R \quad (3)$$

and

$$\delta^{13}\text{C}_R F_R = \delta^{13}\text{C}_{\text{plant}} F_{\text{plant}} + \delta^{13}\text{C}_{\text{SOM}} F_{\text{SOM}} \quad (4)$$

where  $\delta^{13}\text{C} = \left[ \left( \frac{^{13}\text{C}/^{12}\text{C}}{^{13}\text{C}/^{12}\text{C}} \right)_{\text{sample}} / \left( \frac{^{13}\text{C}/^{12}\text{C}}{^{13}\text{C}/^{12}\text{C}} \right)_{\text{standard}} - 1 \right] \times 1000$ ,  $\delta^{13}\text{C}_{\text{plant}}$  and  $\delta^{13}\text{C}_{\text{SOM}}$  are the plant and SOM end-member values, and  $f_{\text{plant}}$  and  $f_{\text{SOM}}$  are the proportion of the total flux attributable to plant or SOM sources, respectively. Combining Equations (1)–(4) and rearranging gives

$$f_{\text{SOM}} = (\delta^{13}\text{C}_R - \delta^{13}\text{C}_{\text{plant}}) / (\delta^{13}\text{C}_{\text{SOM}} - \delta^{13}\text{C}_{\text{plant}}) \quad (5)$$

and

$$f_{\text{plant}} = 1 - f_{\text{SOM}} \quad (6)$$

### 2.2 | End-member measurements

#### 2.2.1 | From plant and soil dry matter

For the  $\delta^{13}\text{C}$  of plant material, grass shoot clippings were taken on 3–4 October 2019 from six randomly selected lysimeters. The samples were dried at 65°C to constant weight and ground in a planetary ball-mill (Fritsch Pulverisette 6, Gerhardt, Brackley, UK) for 6 min at 300 rpm. The samples were analysed for  $\delta^{13}\text{C}$  by combustion using a Delta<sup>Plus</sup> XP IRMS connected via a Conflo III to a Flash EA 1112 Series Elemental Analyser (all Thermo Finnigan, Bremen, Germany). Six replicate sub-samples from each sampled lysimeter were analysed.

For  $\delta^{13}\text{C}$  of soil material, bulk soil was sampled in April 2018 (before seeding with *B. dactyloides*) by taking 2-cm diameter cores to 10-cm depth with a stainless steel auger. Ten samples were taken from each of four randomly selected lysimeters, air dried and bulked for each lysimeter. Sub-samples of the soil were ground using a pestle and mortar to pass a 2 mm sieve and analysed by combustion as for the plant material.

#### 2.2.2 | From respiration

For the  $\delta^{13}\text{C}$  of soil flux, air-dry samples of the original field soil, unexposed to the C<sub>4</sub> grass, were moistened to field capacity, packed to a depth of 3 cm in 15-cm internal diameter plastic pipes with acrylic disks glued to their bases, and incubated for 41 days at ambient laboratory temperature. A pneumatically-operated gas flux chamber (eosAC, Eosense, Nova Scotia, Canada) was fitted on top, and connected to a Picarro G2201-*i* analyser via a multiplexer (eosMX, Eosense) and Picarro A0702 diaphragm pump. Measurements of CO<sub>2</sub> respired and its  $\delta^{13}\text{C}$  were taken over 22 min and  $\delta^{13}\text{C}_{\text{SOM}}$  obtained using Keeling

plots. Two replicate mesocosms were used, with seven repeated measurements per mesocosm.

For the  $\delta^{13}\text{C}$  of plant flux, seeds of *B. dactyloides* were germinated and sown in moist sand that had been heat treated to remove organic matter and packed into plastic pipes as for the  $\delta^{13}\text{C}_{\text{SOM}}$  measurements. The grass was then grown for 2 months in a glasshouse under ambient summer lighting with watering to constant weight. Respiration measurements were made by bringing the mesocosms into an indoor laboratory and attaching flux chambers over the grass in the dark as for the  $\delta^{13}\text{C}_{\text{SOM}}$  measurements, with a 17 min measurement period, and  $\delta^{13}\text{C}_{\text{plant}}$  was obtained using Keeling plots. Three replicate mesocosms were used, with four repeated measurements per mesocosm.

## 2.3 | Sensitivity analysis

To assess the effect of variation or uncertainty in end-member values, we conducted a sensitivity analysis using flux data gathered as above over periods when the grass was actively growing (2–7 August 2018). We partitioned the measured fluxes using end-member values spanning the ranges presented in Figure 1:  $\delta^{13}\text{C}_{\text{SOM}} = -21\text{‰}$ ,  $-24\text{‰}$ ,  $-27\text{‰}$  and  $-30\text{‰}$  with  $\delta^{13}\text{C}_{\text{plant}} = -14.2\text{‰}$  (as measured on dry plant material); and  $\delta^{13}\text{C}_{\text{plant}} = -10\text{‰}$ ,  $-12\text{‰}$ ,  $-14\text{‰}$ , and  $-16\text{‰}$  with  $\delta^{13}\text{C}_{\text{SOM}} = -28.8\text{‰}$  (as measured on dry soil material). We calculated daily means, maxima and minima of  $F_{\text{SOM}}$  and  $F_{\text{plant}}$  over the measurement periods for all  $\delta^{13}\text{C}_{\text{SOM}}$  and  $\delta^{13}\text{C}_{\text{plant}}$  values. Data analysis was conducted using R version 3.5.1 (R Core Team, 2017).

To assess the effect of a diurnal shift in  $\delta^{13}\text{C}_{\text{plant}}$  in partitioning flux data, we compared a fixed  $\delta^{13}\text{C}_{\text{plant}} = -14.2\text{‰}$  (as measured on dry plant material) with a value enriched under light conditions by  $3\text{‰}$  (based on the  $2\text{‰}$ – $4\text{‰}$  variation discussed in Introduction), both with fixed  $\delta^{13}\text{C}_{\text{SOM}} = -28.8\text{‰}$  (as measured on dry soil material). For simplicity, the plant end-member was treated as either the dark or light value, without a gradual transition. We also tested the effect of more gradual diurnal variation with simulated sinusoidal changes in  $F_{\text{R}}$ ,  $\delta^{13}\text{C}_{\text{R}}$  and  $\delta^{13}\text{C}_{\text{plant}}$  with peaks at midday. We reason that the  $\delta^{13}\text{C}_{\text{plant}}$  of night-time respiration will more-closely track the long-term average value, indicated by the dry plant matter value, and the day-time value will represent the perturbation caused by altered substrate availability and metabolite partitioning during photosynthesis. Day-time conditions were defined as when incoming solar radiation  $\geq 0.05 \text{ W m}^{-2} \text{ nm}^{-1}$ , as measured by a weather station (Vaisala WXT520) on the site. In principle, it would be possible to systematically fit a variable end-member

value to the data set using model-data fusion techniques. We have not done so because the objective of this study is to illustrate the importance of allowing for time-varying end-members, rather than a broader exploration of model-data fusion methods.

Total daily SOM respiration for each day over the growing season was found by fitting a natural cubic spline to the measured data and calculating the area under the resulting curve. Days for which  $>6$  measurements (out of the target 36) were missed (because of photosynthesis measurements, system maintenance or other reasons) were excluded. Cumulative SOM respiration over the season was then found by fitting a cubic spline to the daily SOM respiration data obtained.

## 3 | RESULTS

### 3.1 | Measured respiration and $\delta^{13}\text{C}_{\text{R}}$

Diurnal patterns in both total flux magnitude and  $\delta^{13}\text{C}$  were found for plant and soil respiration (Figure 2). In July (when the grass sward was still becoming established) and August (when grass growth was most active), diurnal patterns in both the total flux magnitude and its  $\delta^{13}\text{C}$  are clear, with  $\delta^{13}\text{C}$  values higher in August than July. In December (when the grass was dormant), the fluxes are smaller, and there are no clear diurnal patterns to either the total flux or its  $\delta^{13}\text{C}$ . In July and August, the respiration flux peaks after midday, matching diurnal variation in solar radiation and air temperature (Figure 3). The  $\delta^{13}\text{C}$  of respiration also peaks after midday with a maximum value  $2\text{‰}$ – $4\text{‰}$  less negative than the night-time minimum.

### 3.2 | End-member values

The  $\delta^{13}\text{C}_{\text{plant}}$  values measured from night-time respiration were  $<1\text{‰}$  more negative than those from plant dry matter (Table 1). The  $\text{C}_3$  soil material had  $\delta^{13}\text{C}$  approximately  $16\text{‰}$  more negative (i.e., more  $^{13}\text{C}$  depleted) than the plant material. The  $\delta^{13}\text{C}_{\text{SOM}}$  values measured from respiration fluxes were approximately  $2\text{‰}$  more negative than those from bulk soil material. These differences in  $\delta^{13}\text{C}_{\text{plant}}$  and  $\delta^{13}\text{C}_{\text{SOM}}$  between dry matter and respiration methods are within ranges expected for transient processes driven by environmental variability, as well as artificial biases between the methods. Based on the dry matter values averaging over transient variations, we take these as the standard values for the sensitivity analysis.



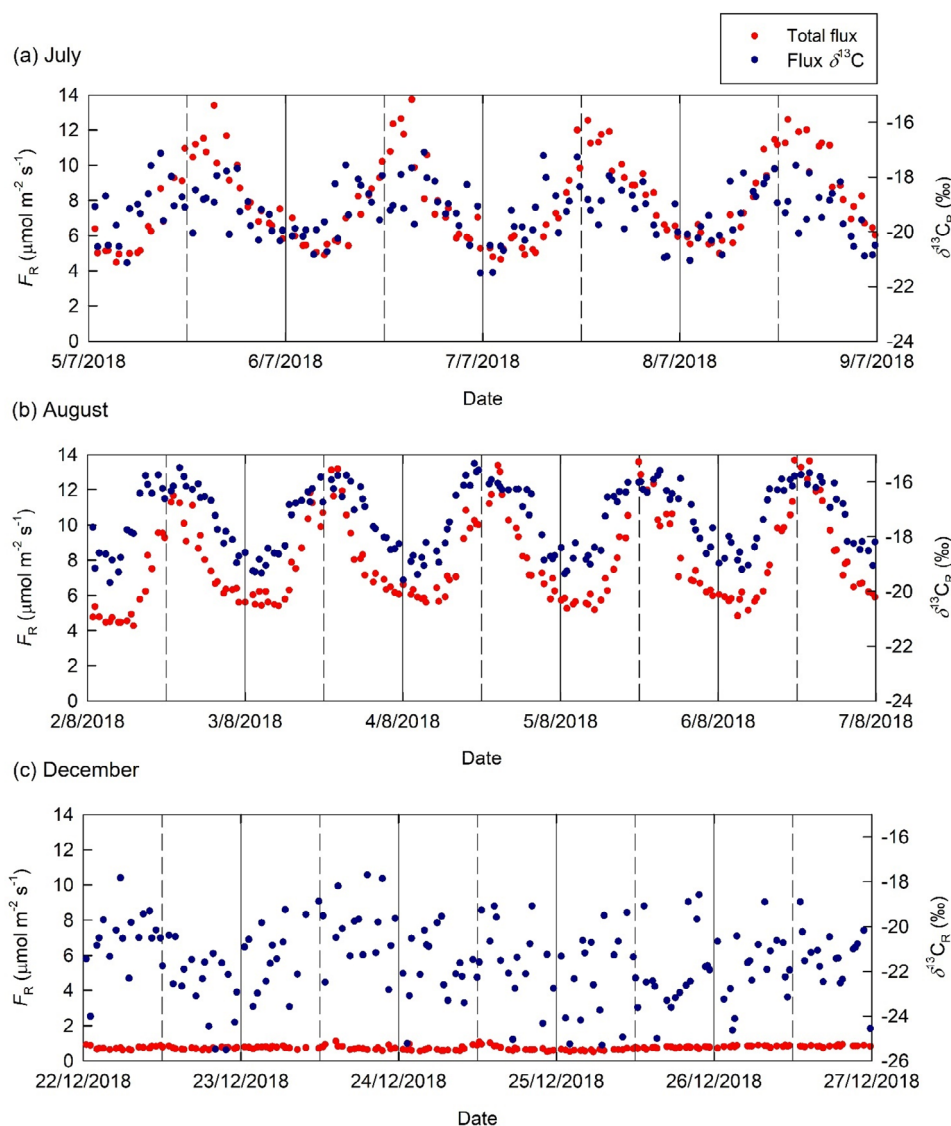


**FIGURE 2** Total plant and soil  $\text{CO}_2$  fluxes and their  $\delta^{13}\text{C}$  signatures from (a) 5–9 July, (b) 2–7 August and (c) 22–27 December 2018. Data are measurements from 12 lysimeters, each measured thrice daily; individual points represent a measurement from a single lysimeter. Solid lines indicate midnight; dashed lines indicate midday

### 3.3 | Sensitivity analysis

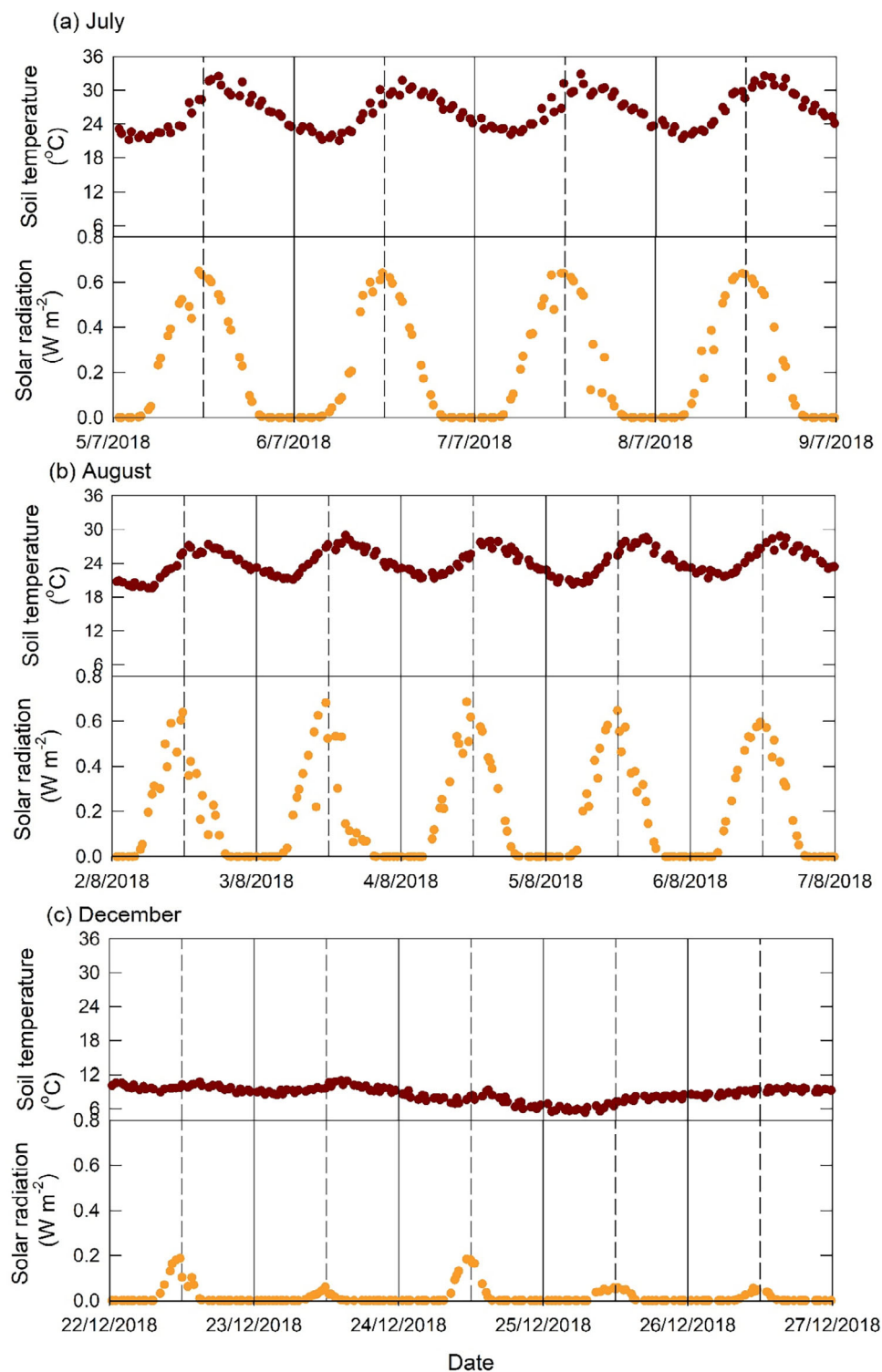
The sensitivities of partitioned plant and soil fluxes to  $\delta^{13}\text{C}_{\text{plant}}$  and  $\delta^{13}\text{C}_{\text{SOM}}$  in early August (when grass growth was greatest) are shown in Figure 4. The daily mean, minimum and maximum fluxes averaged over the measurement period are shown, with  $\delta^{13}\text{C}_{\text{plant}}$  and  $\delta^{13}\text{C}_{\text{SOM}}$  values varied over the ranges indicated in Figure 1. In this period, the apparent  $F_{\text{plant}}$  values are up to an order of magnitude greater than  $F_{\text{SOM}}$ , depending on the end-member values. The difference decreases as growth declines and in December mean  $F_{\text{SOM}}$  is greater than mean  $F_{\text{plant}}$  at most end-member values tested (Supporting information Figure S1).

The effects of end-member values depend on how far they differ from  $\delta^{13}\text{C}_R$ . Since in most cases  $\delta^{13}\text{C}_{\text{SOM}} < \delta^{13}\text{C}_R < \delta^{13}\text{C}_{\text{plant}}$ , it follows from Equation (5) that increasing  $\delta^{13}\text{C}_{\text{SOM}}$  with  $\delta^{13}\text{C}_{\text{plant}}$  constant, and increasing  $\delta^{13}\text{C}_{\text{plant}}$  with  $\delta^{13}\text{C}_{\text{SOM}}$  constant, both result in an increase in  $f_{\text{SOM}}$ , that is

a greater proportion of the flux comes from the soil. However, where  $\delta^{13}\text{C}_{\text{SOM}}$  is more enriched than  $\delta^{13}\text{C}_R$  the calculated  $F_{\text{plant}}$  is negative, and vice versa. Negative night-time respiration fluxes are impossible, so this can be used to constrain the possible bounds of  $\delta^{13}\text{C}_{\text{SOM}}$  and  $\delta^{13}\text{C}_{\text{plant}}$ . From Figure 4 this limits  $\delta^{13}\text{C}_{\text{SOM}}$  in our system to values more depleted than approximately  $-25\text{‰}$  and  $\delta^{13}\text{C}_{\text{plant}}$  to values more enriched than approximately  $-15.5\text{‰}$ .

Diurnal trends in simulated SOM fluxes were found to be substantially affected by a diurnal shift in the plant  $\delta^{13}\text{C}$  end-member on simulated SOM fluxes (Figure 5). For simplicity, the diurnal changes in  $F_R$ ,  $\delta^{13}\text{C}_R$  and  $\delta^{13}\text{C}_{\text{plant}}$  are sinusoidal with midday peaks and midnight troughs, and the maximum and minimum  $F_R$  and  $\delta^{13}\text{C}_R$  values are set to be similar to those for August in Figure 2. It will be seen that with no day-night shift in  $\delta^{13}\text{C}_{\text{plant}}$ , the SOM flux reaches a minimum at midday as  $\delta^{13}\text{C}_R$  peaks, in spite of the peak in  $F_R$ . This would require some

**FIGURE 3** Diurnal changes in solar radiation and temperature from (a) 5–9 July and (b) 2–7 August 2018. Temperature data are measurements from 12 lysimeters measured thrice daily; individual points represent a measurement from a single lysimeter. Solid lines indicate midnight; dashed lines indicate midday



negative priming effect, offsetting the expected daytime increase in  $F_{\text{SOM}}$  with temperature, so is not realistic. However, Figure 5 shows that with a day-time increase in  $\delta^{13}\text{C}_{\text{plant}}$  of at least  $+1\text{‰}$ , which is consistent with literature values (Introduction), there is a more-realistic day-time peak in  $F_{\text{SOM}}$ . The impact of a diurnally varying  $\delta^{13}\text{C}_{\text{plant}}$  is substantial, with a  $3\text{‰}$  shift resulting in a 44% higher daily SOM flux. The SOM fluxes for  $0\text{‰}$ ,  $+1\text{‰}$ ,

$+3\text{‰}$  and  $+5\text{‰}$  shifts in Figure 5 are 3.79, 4.41, 5.47 and  $6.36 \mu\text{mol m}^{-2} \text{d}^{-1}$ , respectively. This suggests an upper bound to the underestimation of diel SOM of approximately 40%. Clear diurnal patterns in both plant and SOM fluxes are evident in July using fixed  $\delta^{13}\text{C}_{\text{plant}}$  and  $\delta^{13}\text{C}_{\text{SOM}}$  values equal to the dry matter values ( $-14.2\text{‰}$  and  $-28.8\text{‰}$ , respectively), with both fluxes peaking after midday (Figure 7). However in August, when plant

growth and respiration are greater, there is little diurnal variation in SOM fluxes, with small peaks around mid-night, though the plant fluxes show the same diurnal pattern as in July and peak after midday. In December, both fluxes are small without clear diurnal trends.

Comparing fluxes partitioned using a fixed plant end-member (Figure 6a–c) with those using a diurnal change in  $\delta^{13}\text{C}_{\text{plant}}$  of 3‰ (Figure 6d–f), it is clear that the former results in an underestimation of the SOM flux, and an overestimation of the plant flux. These differences are largest when the system is dominated by plant respiration. Once the diurnal enrichment of  $\delta^{13}\text{C}_{\text{plant}}$  is accounted for, plant and SOM fluxes in August show

**TABLE 1** Plant and soil end-member  $\delta^{13}\text{C}$  values from flux measurements and analyses of dry matter

Measurement method	<i>n</i>	$\delta^{13}\text{C}$ (‰)
Plant flux	3 (4)	$-15.3 \pm 0.2$
Plant material	6 (1)	$-14.2 \pm 0.0$
Soil flux	2 (7)	$-30.9 \pm 0.1$
Soil material	4 (1)	$-28.8 \pm 0.1$

Note: Data are means  $\pm$  SE (details in Materials and methods). *n* values given are number of samples; in brackets is the number of measurements made from each sample.

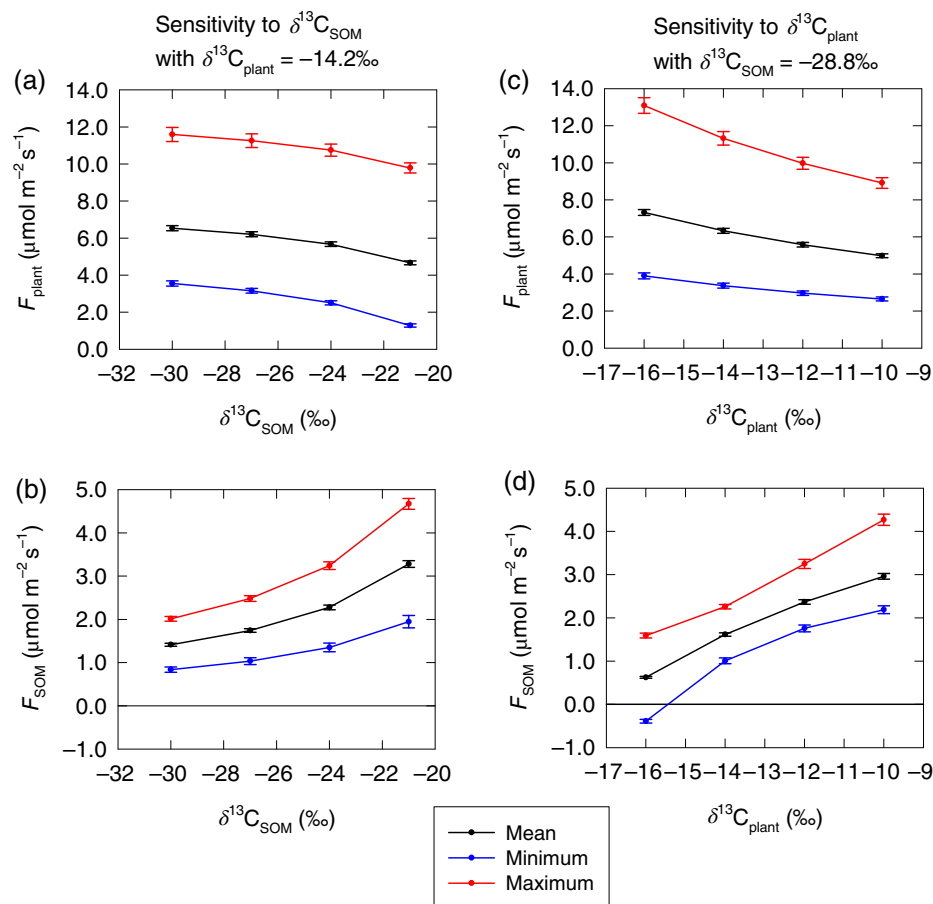


**FIGURE 4** Sensitivity of partitioned plant and soil organic matter (SOM) C fluxes over 2–7 August 2018 to end-member values. Daily mean, minimum and maximum values averaged over the measurement period are shown. Left-hand panels (a, b) show sensitivity to  $\delta^{13}\text{C}_{\text{SOM}}$  at the  $\delta^{13}\text{C}_{\text{plant}}$  measured on plant material; right-hand panels (c, d) show sensitivity to  $\delta^{13}\text{C}_{\text{plant}}$  at the  $\delta^{13}\text{C}_{\text{SOM}}$  measured on soil material. The mean total flux  $\delta^{13}\text{C}$  over this period was  $-17.3 \pm 0.1\text{‰}$ . Data are means  $\pm$  SE

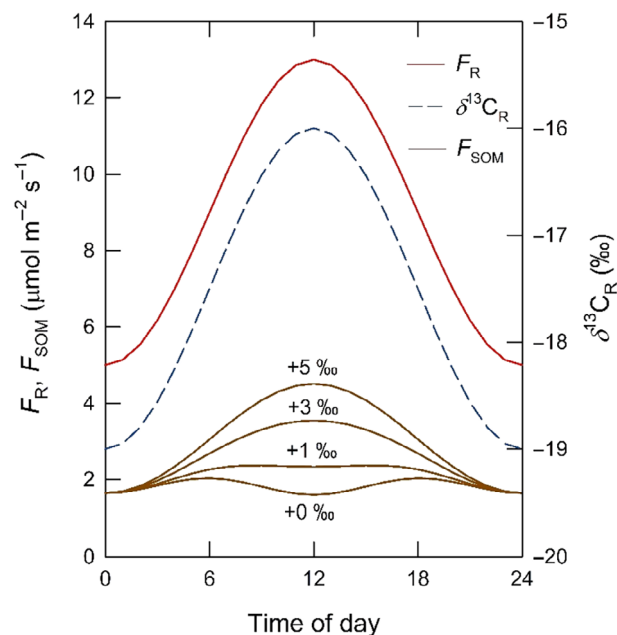


**FIGURE 5** Simulated sensitivity of soil organic matter (SOM) C flux ( $F_{\text{SOM}}$ ) to a night-day shift in the plant end-member ( $\delta^{13}\text{C}_{\text{plant}}$ ; numbers on curves). The diurnal variation in total C flux ( $F_{\text{R}}$ ), its isotope signature ( $\delta^{13}\text{C}_{\text{R}}$ ) and  $\delta^{13}\text{C}_{\text{plant}}$  are simulated as sinusoidal with peaks at midday. The soil end-member is constant, and  $F_{\text{SOM}}$  is calculated with Equations (3) and (5)



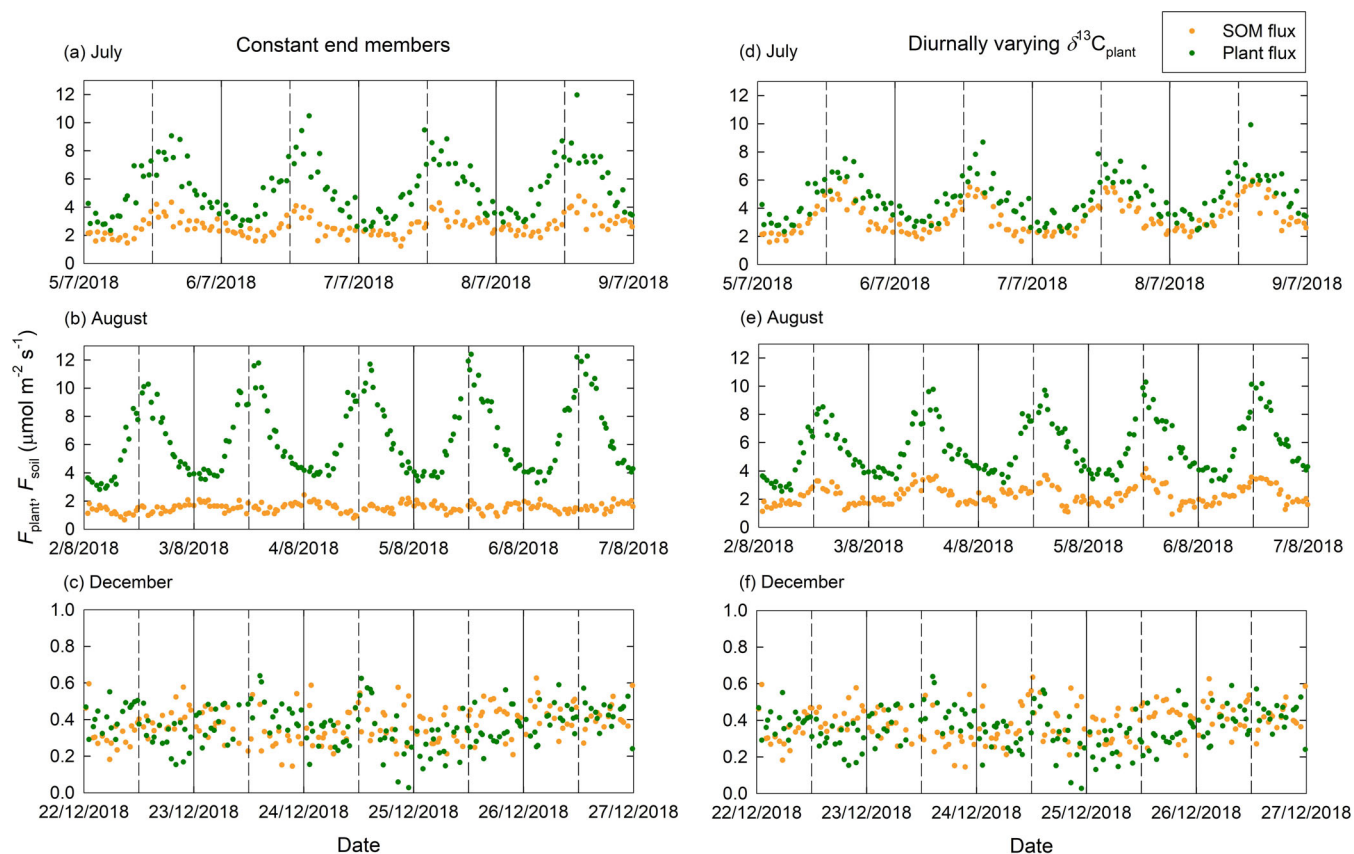


**FIGURE 6** Partitioned plant and soil organic matter (SOM) C fluxes with  $\delta^{13}\text{C}_{\text{SOM}} = -28.8\text{‰}$  and (a–c)  $\delta^{13}\text{C}_{\text{plant}} = -14.2\text{‰}$  or (d–f) a  $+3\text{‰}$  daytime shift in  $\delta^{13}\text{C}_{\text{plant}}$  ( $-14.2\text{‰}$  at night,  $-11.2\text{‰}$  during the day) from 5–9 July, 2–7 August and 22–27 December 2018, respectively. Data are measurements from 12 lysimeters, and each measured thrice daily; individual points represent a measurement from a single lysimeter. Solid lines indicate midnight; dashed lines indicate midday

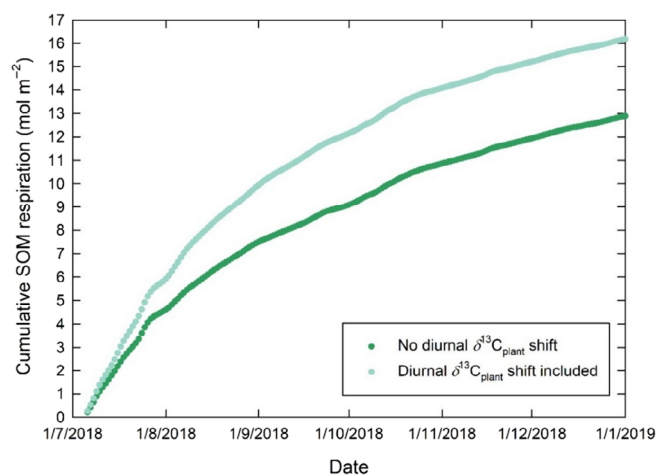


**FIGURE 7** Effect of allowing for a  $+3\text{‰}$  diurnal shift in the plant  $\delta^{13}\text{C}$  end-member on cumulative soil organic matter (SOM) respiration over the 2018 growing season

similar patterns to those in July, with peaks in both fluxes after midday. Increased  $f_{\text{SOM}}$  with the less negative day-time  $\delta^{13}\text{C}_{\text{plant}}$  is expected from Equation (5). We also

found, with fixed  $\delta^{13}\text{C}_{\text{SOM}} = -28.8\text{‰}$  and  $\delta^{13}\text{C}_{\text{plant}} = -11.2\text{‰}$ , the diurnal plant and SOM respiration patterns in July and August were aligned, both peaking after midday (Supporting information Figure S2). The main changes compared to Figure 6 are that in July, the night-time SOM and plant fluxes are roughly equal; in August, the diurnal variation in the SOM flux is reduced; and in December, the SOM flux is generally greater than the plant flux, rather than roughly equal. Allowing for a diurnal shift in  $\delta^{13}\text{C}_{\text{plant}}$  on the cumulative SOM respiration over the 2018 growing season has a substantial effect, increasing total SOM respiration by 26% from July to December (Figure 7). The majority of this difference occurred between mid-July and mid-September, when plant respiration was most dominant.

## 4 | DISCUSSION

### 4.1 | Effects of varying end-members

Our results show that allowing for a diurnally varying plant end-member produces large differences in apparent

SOM turnover on diurnal and seasonal time scales, and an apparent tight coupling with photosynthesis. Although changes in end-members are to be expected with variations in light intensity, temperature, moisture and other variables (Introduction), we believe this is the first study to quantify the consequences for partitioning of plant and soil C fluxes under field conditions. We have focused on the plant end-member because there are necessarily large diurnal changes in it—of the order of 1‰–5‰—driven by changes in light intensity in both  $C_3$  and  $C_4$  plants (Barbour et al., 2005; Sun et al., 2010; Tcherkez et al., 2003; Zhong et al., 2017). In our system, not accounting for this diurnal variation resulted in underestimation of SOM turnover by 26% over 6 months, or up to 40% per day during the height of the growing season.

The effect of diurnal  $\delta^{13}C_{\text{plant}}$  changes varies with plant growth over the season. In early July, when the grass sward was still becoming established, clear diurnal patterns in total C flux, its  $\delta^{13}C$  and the SOM flux obtained with or without a varying plant end-member were apparent, along with strong diurnal variation in solar radiation and temperature. During this period, the SOM flux obtained with fixed end-member values measured on plant and soil dry matter was comparable to the plant flux, and a diurnal pattern in SOM fluxes was evident with a peak after midday. This is the expected pattern due to the well-established effects of diurnal changes in temperature on plant and soil respiration (Phillips et al., 2011; Vargas et al., 2011). However in August, when the grass sward was better established and plant respiration a much larger proportion of the total C flux, there was little apparent diurnal variation in SOM turnover if the end-members were constant. From the expected effect of diurnally varying temperature, and our July results, these apparent August SOM fluxes are evidently erroneous. We obtained a more realistic diurnal pattern when we allowed for a diurnally-varying plant end-member.

The grass sward was not fully established in July, but it was well established in August, and the plant flux was a substantially larger proportion of the net flux. The distortions of partitioned SOM fluxes in August but not July were thus due to the greater dominance of plant respiration. The daytime increase in the measured  $^{13}C$  enrichment of the total flux results in an exaggerated partitioning in favour of the plant flux. With increasing dominance by the plant flux, this distorts flux partitioning to the point that daytime SOM flux peaks disappears or even becomes inverted, as we saw in the sensitivity analyses. As a  $^{13}C$  enrichment of both  $C_3$  and  $C_4$  respiration during photosynthesis is expected (Introduction), we consider not allowing for it to be the likely cause of the inverted SOM flux peaks we observed in August.

## 4.2 | Alternative explanations for diurnal patterns

An alternative explanation is that the real plant end-member, while stable over diurnal timescales, was more  $^{13}C$  enriched than the value we used. We also reproduced the daytime SOM respiration peak with a fixed plant end-member more  $^{13}C$ -enriched than the measured dry matter value by 3‰. However, we see no reason why the measurement of  $\delta^{13}C_{\text{plant}}$  in dry matter should misrepresent the long-term average  $\delta^{13}C_{\text{plant}}$  to this extent, given that the plant flux measured under dark conditions was less enriched than the dry matter measurement.

No daytime increase in SOM flux, in spite of the daytime soil warming, might be expected if soil microbes preferentially used root exudates rather than SOM as their carbon source, as root exudation increases during the day (Bahn et al., 2009). Against this, SOM turnover may be enhanced by priming effects of root exudates, whereby exudates provide energy for microbes to ‘mine’ limiting nutrients from SOM (Paterson et al., 2009; Werth & Kuzyakov, 2010). Therefore, a daytime increase in SOM flux is expected both due to the effects of daytime warming and priming effects. The fact that the post-midday peaks in SOM flux (Figure 6) closely match the peaks in solar radiation (Figure 3), and more closely than the peaks in soil temperature which occur earlier in the day (Figure 3), suggests a tight coupling between solar radiation and the SOM flux. To the extent that root exudation varies closely with solar radiation (Bahn et al., 2009; Kuzyakov & Gavrichkova, 2010), this is good evidence for priming effects. We conclude that a diurnally varying SOM-flux linked to a diurnally varying plant end-member is more consistent with theoretical expectations than a diurnally constant SOM flux.

In our system, both above- and below-ground respiration are measured, and so plant respiration is the predominant component during the main growing season. Errors in  $\delta^{13}C_{\text{plant}}$  have a correspondingly large effect on the calculated SOM flux. This effect will be less in systems that exclude above-ground respiration. However, it is nonetheless necessary to allow for diurnal shifts in the plant end-member as root respiration and exudation vary diurnally with photosynthesis (Bahn et al., 2009; Kuzyakov & Gavrichkova, 2010).

## 4.3 | Implications for measuring SOM turnover

How should temporal changes in end-members be quantified and allowed for? Baseline end-members can be characterised either by directly sampling respiration

fluxes or by measuring the  $\delta^{13}\text{C}$  of plant and soil dry matter. The  $\delta^{13}\text{C}$  of dry matter, produced during varying environmental conditions, provides a long-term integration of temporal variation (Cernusak et al., 2013). This applies to both the plant end-member, which is particularly subject to variation with light intensity as we have seen, and the soil end-member, which is particularly subject to variation with recent C inputs, which make up only a small fraction of the total soil C. A more systematic approach is to use model-data fusion methods to fit variable end-members to a data set gathered across a growing season, parsimoniously selecting parameters consistent with the full data set (Ogle & Pendall, 2015; Phillips et al., 2017). Prior values of end-members for this can be set using the  $\delta^{13}\text{C}$  of plant and soil dry-matter samples.

We have shown that allowing for short-term variation in flux partitioning is important for correctly quantifying daily and seasonal patterns in SOM fluxes. Information at such time-scales is needed to explore biotic and abiotic processes controlling SOM dynamics, particularly root-soil-microbe interactions and priming effects. Until recently, such processes have not been well represented in SOM models, but the need to do so is widely discussed (Wieder et al., 2015). Inclusion of priming effects in SOM models results in qualitatively different medium and long-term predictions, including at global scales (Guenet et al., 2018; Woof & Lehmann, 2019; Wutzler et al., 2017). However, progress in defining minimal models for these purposes is constrained by the availability of reliable data on priming and other effects under field conditions. The points discussed here need to be allowed for in using isotope fractionation methods to obtain such data.

## 5 | CONCLUSIONS

1. There is necessarily transient variation in plant and soil  $\delta^{13}\text{C}$  end-members over the course of a growing season and on diurnal timescales, due to varying environmental conditions. Large diurnal variation in the plant end-member is well established, but is generally not accounted for when using  $\delta^{13}\text{C}$  to partition soil and plant fluxes.
2. In our experiments, not allowing for diurnal variation in the plant end-member caused partitioning errors of 26% over a season and 40% over a day during periods of high plant growth.
3. Potential errors are greatest when the end-member is far from  $\delta^{13}\text{C}$  of the total flux, or the total flux is small, so that a small change in flux has a proportionally greater effect.

## ACKNOWLEDGEMENTS

The field laboratory was built with a Royal Society Wolfson Laboratory Refurbishment Grant (WL080021/Kirk). The CRDS analyser was provided by the Agri-Epi Centre, Cranfield Hub. Christopher S. McCloskey was supported by the Soils Training and Research Studentships (STARS) Centre for Doctoral Training, funded by the Biotechnology and Biological Sciences Research Council and the Natural Environment Research Council (grant number NE-M009106-1). The James Hutton Institute receives funding from the Rural and Environment Science and Analytical Services Division (RESAS) of the Scottish Government.

## CONFLICT OF INTEREST

The authors have no conflicts of interest related to the work presented in this manuscript.

## AUTHOR CONTRIBUTIONS

**Christopher McCloskey:** Conceptualisation (equal); data curation (lead); formal analysis (lead); investigation (equal); methodology (equal); writing – original draft (lead); writing – review and editing (equal). **Wilfred Otten:** Conceptualisation (equal); investigation (equal); supervision (equal); writing – review and editing (equal). **Eric Paterson:** Conceptualisation (equal); investigation (equal); supervision (equal); writing – review and editing (equal). **Guy Kirk:** Conceptualisation (equal); funding acquisition (lead); investigation (equal); methodology (equal); project administration (lead); resources (lead); supervision (equal); writing – original draft (equal); writing – review and editing (equal).

## DATA AVAILABILITY STATEMENT

The data used in this is available at CORD c/o the Cranfield University Library, <https://doi.org/10.17862/cranfield.rd.16836889>.

## ORCID

Christopher S. McCloskey  <https://orcid.org/0000-0002-4439-8263>

Wilfred Otten  <https://orcid.org/0000-0002-3847-9825>

Eric Paterson  <https://orcid.org/0000-0003-1512-7787>

Guy J. D. Kirk  <https://orcid.org/0000-0002-7739-9772>

## REFERENCES

- Bahn, M., Schmitt, M., Siegwolf, R., Richter, A., & Brüggemann, N. (2009). Does photosynthesis affect grassland soil-respired  $\text{CO}_2$  and its carbon isotope composition on a diurnal timescale? *New Phytologist*, 182, 451–460.
- Balesdent, J., Mariotti, A., & Guillet, B. (1987). Natural  $^{13}\text{C}$  abundance as a tracer for studies of soil organic matter dynamics. *Soil Biology & Biogeochemistry*, 19, 25–30.

- Barbour, M. M., Hunt, J. E., Dungan, R. J., Turnbull, M. H., Brailsford, G. W., Farquhar, G. D., & Whitehead, D. (2005). Variation in the degree of coupling between  $\delta^{13}\text{C}$  of phloem sap and ecosystem respiration in two mature *Nothofagus* forests. *New Phytologist*, 166, 497–512.
- Boström, B., Comstedt, D., & Ekblad, A. (2007). Isotope fractionation and  $^{13}\text{C}$  enrichment in soil profiles during the decomposition of soil organic matter. *Oecologia*, 153, 89–98.
- Bowling, D. R., McDowell, N. G., Bond, B. J., Law, B. E., & Ehleringer, J. R. (2002).  $^{13}\text{C}$  content of ecosystem respiration is linked to precipitation and vapor pressure deficit. *Oecologia*, 131, 113–124.
- Bowling, D. R., Pataki, D. E., & Ehleringer, J. R. (2003). Critical evaluation of micrometeorological methods for measuring ecosystem–atmosphere isotopic exchange of  $\text{CO}_2$ . *Agricultural and Forest Meteorology*, 116, 159–179.
- Bowling, D. R., Pataki, D. E., & Randerson, J. T. (2008). Carbon isotopes in terrestrial ecosystem pools and  $\text{CO}_2$  fluxes. *New Phytologist*, 178, 24–40.
- Brüggemann, N., Gessler, A., Kayler, Z., Keel, S., Badeck, F., Barthel, M., Boeckx, P., Buchmann, N., Brugnoli, E., & Esperschütz, J. (2011). Carbon allocation and carbon isotope fluxes in the plant–soil–atmosphere continuum: A review. *Bio-geosciences*, 8, 3457–3489.
- Buchmann, N., Guehl, J.-M., Barigah, T. S., & Ehleringer, J. R. (1997). Interseasonal comparison of  $\text{CO}_2$  concentrations, isotopic composition, and carbon dynamics in an Amazonian rainforest (French Guiana). *Oecologia*, 110, 120–131.
- Cernusak, L. A., Ubierna, N., Winter, K., Holtum, J. A. M., Marshall, J. D., & Farquhar, G. D. (2013). Environmental and physiological determinants of carbon isotope discrimination in terrestrial plants. *New Phytologist*, 200, 950–965.
- Cornwell, W. K., Wright, I. J., Turner, J., Maire, V., Barbour, M. M., Cernusak, L. A., Dawson, T., Ellsworth, D., Farquhar, G. D., Griffiths, H., Keitel, C., Knohl, A., Reich, P. B., Williams, D. G., Bhaskar, R., Cornelissen, J. H. C., Richards, A., Schmidt, S., Valladares, F., ... Santiago, L. S. (2018). Climate and soils together regulate photosynthetic carbon isotope discrimination within  $\text{C}_3$  plants worldwide. *Global Ecology and Biogeography*, 27, 1056–1067.
- Farquhar, G. D., Ehleringer, J. R., & Hubick, K. T. (1989). Carbon isotope discrimination and photosynthesis. *Annual Review of Plant Physiology and Plant Molecular Biology*, 40, 503–537.
- Fassbinder, J. J., Griffis, J. J., & Baker, J. M. (2012). Evaluation of carbon isotope flux partitioning theory under simplified and controlled environmental conditions. *Agricultural and Forest Meteorology*, 153, 154–164.
- Fessenden, J. E., & Ehleringer, J. R. (2003). Temporal variation in  $\delta^{13}\text{C}$  of ecosystem respiration in the Pacific northwest: Links to moisture stress. *Oecologia*, 136, 129–136.
- Flanagan, L. B., Brooks, J. R., Varney, G. T., Berry, S. C., & Ehleringer, J. R. (1996). Carbon isotope discrimination during photosynthesis and the isotope ratio of respired  $\text{CO}_2$  in boreal forest ecosystems. *Global Biogeochemical Cycles*, 10, 629–640.
- Fu, S., & Cheng, W. (2002). Rhizosphere priming effects on the decomposition of soil organic matter in  $\text{C}_4$  and  $\text{C}_3$  grassland soils. *Plant and Soil*, 238, 289–294.
- Ghannoum, O., von Caemmerer, S., & Conroy, J. P. (2002). The effect of drought on plant water use efficiency of nine NAD–ME and nine NADP–ME Australian  $\text{C}_4$  grasses. *Functional Plant Biology*, 29, 1337–1348.
- Ghashghaie, J., & Badeck, F. W. (2014). Opposite carbon isotope discrimination during dark respiration in leaves versus roots – A review. *New Phytologist*, 201, 751–769.
- Guenet, B., Camino-Serrano, M., Ciais, P., Tifafi, M., Maignan, F., Soong, J. L., & Janssens, I. A. (2018). Impact of priming on global soil carbon stocks. *Global Change Biology*, 4, 1873–1883.
- Hartmann, H., Bahn, M., Carbone, M., & Richardson, A. D. (2020). Plant carbon allocation in a changing world – Challenges and progress: Introduction to a virtual issue on carbon allocation. *New Phytologist*, 227, 981–988.
- Hattersley, P. W. (1982).  $\delta^{13}\text{C}$  values of  $\text{C}_4$  types in grasses. *Functional Plant Biology*, 9, 139–154.
- Hemming, D., Yakir, D., Ambus, P., Aurela, M., Besson, C., Black, K., Buchmann, N., Burlett, R., Cescatti, A., Clement, R., Gross, P., Granier, A., Grunwald, T., Havrankova, K., Janous, D., Janssens, I. A., Knohl, A., Ostner, B. K., Kowalski, A., ... Vesala, T. (2005). Pan-European  $\delta^{13}\text{C}$  values of air and organic matter from forest ecosystems. *Global Change Biology*, 11, 1065–1093.
- Hobbie, E. A., Macko, S., & Shugart, H. (1999). Insights into nitrogen and carbon dynamics of ectomycorrhizal and saprotrophic fungi from isotopic evidence. *Oecologia*, 118, 353–360.
- Hobbie, E. A., Weber, N. S., & Trappe, J. M. (2001). Mycorrhizal vs saprotrophic status of fungi: The isotopic evidence. *New Phytologist*, 150, 601–610.
- Kohzu, A., Yoshioka, T., Ando, T., Takahashi, M., Koba, K., & Wada, E. (1999). Natural  $^{13}\text{C}$  and  $^{15}\text{N}$  abundance of field-collected fungi and their ecological implications. *New Phytologist*, 144, 323–330.
- Kramer, C., & Gleixner, G. (2006). Variable use of plant- and soil-derived carbon by microorganisms in agricultural soils. *Soil Biology & Biochemistry*, 28, 3267–3278.
- Kuzyakov, Y., & Gavrichkova, O. (2010). Time lag between photosynthesis and carbon dioxide efflux from soil: A review of mechanisms and controls. *Global Change Biology*, 16, 3386–3406.
- Lee, S.-C., Christen, A., Black, T. A., Jassal, R. S., Ketler, R., & Nesic, Z. (2020). Partitioning of net ecosystem exchange into photosynthesis and respiration using continuous stable isotope measurements in a Pacific Northwest Douglas-fir forest ecosystem. *Agricultural and Forest Meteorology*, 292, 108109.
- Lerch, T. Z., Nunan, N., Dignac, M. F., Chenu, C., & Mariotti, A. (2011). Variations in microbial isotopic fractionation during soil organic matter decomposition. *Biogeochemistry*, 106, 5–21.
- Lloyd, D., Ritz, K., Paterson, E., & Kirk, G. J. D. (2016). Effects of soil type and composition of rhizodeposits on rhizosphere priming phenomena. *Soil Biology and Biochemistry*, 103, 512–521.
- McCloskey, C., Otten, W., Paterson, E., Ingram, B., & Kirk, G. J. D. (2020). A field system for measuring plant and soil carbon fluxes using stable isotope methods. *European Journal of Soil Science*. <https://doi.org/10.1111/ejss.13016>
- Millard, P., Midwood, A. J., Hunt, J. E., Whitehead, D., & Boutton, T. W. (2008). Partitioning soil surface  $\text{CO}_2$  efflux into autotrophic and heterotrophic components, using natural gradients in soil  $\delta^{13}\text{C}$  in an undisturbed savannah soil. *Soil Biology & Biochemistry*, 40, 1575–1582.
- Nickerson, N., & Risk, D. (2009). Keeling plots are non-linear in non-steady state diffusive environments. *Geophysical Research Letters*, 36, L08401.



- Ogle, K., & Pendall, E. (2015). Isotope partitioning of soil respiration: A Bayesian solution to accommodate multiple sources of variability. *Journal of Geophysical Research: Biogeosciences*, 120, 221–236.
- Paterson, E., Midwood, A. J., & Millard, P. (2009). Through the eye of the needle: A review of isotope approaches to quantify microbial processes mediating soil carbon balance. *New Phytologist*, 184, 19–33.
- Pausch, J., & Kuzyakov, Y. (2012). Soil organic carbon decomposition from recently added and older sources estimated by  $\delta^{13}\text{C}$  values of  $\text{CO}_2$  and organic matter. *Soil Biology & Biochemistry*, 55, 40–47.
- Phillips, C. L., Bond-Lamberty, B., Desai, A. R., Lavoie, M., Risk, D., Tang, J., Todd-Brown, K., & Vargas, R. (2017). The value of soil respiration measurements for interpreting and modeling terrestrial carbon cycling. *Plant and Soil*, 413, 1–25.
- Phillips, C. L., Nickerson, N., Risk, D., & Bond, B. J. (2011). Interpreting diel hysteresis between soil respiration and temperature. *Global Change Biology*, 17, 515–527.
- R Core Team. (2017). *R: A language and environment for statistical computing*. R Foundation for Statistical Computing.
- Rochette, P., & Flanagan, L. B. (1997). Quantifying rhizosphere respiration in a corn crop under field conditions. *Soil Science Society of America Journal*, 61, 466–474.
- Scartazza, A., Mata, C., Matteucci, G., Yakir, D., Moscatello, S., & Brugnoli, E. (2004). Comparisons of  $\delta^{13}\text{C}$  of photosynthetic products and ecosystem respiratory  $\text{CO}_2$  and their responses to seasonal climate variability. *Oecologia*, 140, 340–351.
- Snell, H. S. K., Robinson, D., & Midwood, A. J. (2014). Minimising methodological biases to improve the accuracy of partitioning soil respiration using natural abundance  $^{13}\text{C}$ . *Rapid Communications in Mass Spectrometry*, 28, 2341–2351.
- Sun, W., Resco, V., & Williams, D. G. (2010). Nocturnal and seasonal patterns of carbon isotope composition of leaf dark-respired carbon dioxide differ among dominant species in a semiarid savanna. *Oecologia*, 164, 297–310.
- Tcherkez, G., Nogues, S., Bleton, J., Cornic, G., Badeck, F., & Ghashghaie, J. (2003). Metabolic origin of carbon isotope composition of leaf dark-respired  $\text{CO}_2$  in French bean. *Plant Physiology*, 131, 237–244.
- Trudell, S. A., Rygielwicz, P. T., & Edmonds, R. L. (2004). Patterns of nitrogen and carbon stable isotope ratios in macrofungi, plants and soils in two old-growth conifer forests. *New Phytologist*, 164, 317–335.
- Vargas, R., Baldocchi, D. D., Bahn, M., Hanson, P. J., Hosman, K. P., Kulmala, L., Pumpanen, K., & Yang, B. (2011). On the multi-temporal correlation between photosynthesis and soil  $\text{CO}_2$  efflux: Reconciling lags and observations. *New Phytologist*, 191, 1006–1017.
- von Caemmerer, S., Ghannoum, O., Pengelly, J. L., & Cousins, A. B. (2014). Carbon isotope discrimination as a tool to explore  $\text{C}_4$  photosynthesis. *Journal of Experimental Botany*, 65, 3459–3470.
- Wang, G., Han, J., Zhou, L., Xiong, X., & Wu, Z. (2005). Carbon isotope ratios of plants and occurrences of  $\text{C}_4$  species under different soil moisture regimes in arid region of Northwest China. *Physiologia Plantarum*, 125, 74–81.
- Wang, X., Tang, C., Severi, J., Butterly, C. R., & Baldock, J. A. (2016). Rhizosphere priming effect on soil organic carbon decomposition under plant species differing in soil acidification and root exudation. *New Phytologist*, 211, 864–873.
- Wedin, D. A., Tieszen, L. L., Dewey, B., & Pastor, J. (1995). Carbon isotope dynamics during grass decomposition and soil organic matter formation. *Ecology*, 76, 1383–1392.
- Wehr, W., & Saleska, S. R. (2015). An improved isotopic method for partitioning net ecosystem-atmosphere  $\text{CO}_2$  exchange. *Agricultural and Forest Meteorology*, 214–215, 515–531.
- Weiguo, L., Xiahong, F., Youfeng, N., Qingle, Z., Yunning, C., & Zhisheng, A. N. (2005).  $\delta^{13}\text{C}$  variation of  $\text{C}_3$  and  $\text{C}_4$  plants across an Asian monsoon rainfall gradient in arid northwestern China. *Global Change Biology*, 11, 1094–1100.
- Werth, M., & Kuzyakov, Y. (2006). Assimilate partitioning affects  $^{13}\text{C}$  C fractionation of recently assimilated carbon in maize. *Plant and Soil*, 284, 319–333.
- Werth, M., & Kuzyakov, Y. (2008). Root-derived carbon in soil respiration and microbial biomass determined by  $^{14}\text{C}$  and  $^{13}\text{C}$ . *Soil Biology & Biochemistry*, 40, 625–637.
- Werth, M., & Kuzyakov, Y. (2009). Three-source partitioning of  $\text{CO}_2$  efflux from maize field soil by  $^{13}\text{C}$  natural abundance. *Journal of Plant Nutrition and Soil Science*, 172, 487–499.
- Werth, M., & Kuzyakov, Y. (2010).  $^{13}\text{C}$  fractionation at the root-microorganisms-soil interface: A review and outlook for partitioning studies. *Soil Biology and Biochemistry*, 42, 1372–1384.
- Wieder, W. R., Allison, S. D., Davidson, E. A., Georgiou, K., Hararuk, O., He, Y., Hopkins, F., Luo, Y., Smith, M. J., Sulman, B., Todd-Brown, K., Wang, Y. P., Xia, J., & Xu, X. (2015). Explicitly representing soil microbial processes in earth system models. *Global Biogeochemical Cycles*, 29, 1782–1800.
- Woof, D., & Lehmann, J. (2019). Microbial models with minimal mineral protection can explain long-term soil organic carbon persistence. *Scientific Reports*, 9, 6522. doi.org/10.1038/s41598-019-43026-8
- Wutzler, T., Zaehle, S., Schrumppf, M., Ahrens, B., & Reichstein, M. (2017). Adaptation of microbial resource allocation affects modelled long term soil organic matter and nutrient cycling. *Soil Biology & Biochemistry*, 115, 322–336.
- Xiao, C., Guenet, B., Zhou, Y., Su, J., & Janssens, I. A. (2015). Priming of soil organic matter decomposition scales linearly with microbial biomass response to litter input in steppe vegetation. *Oikos*, 124, 649–657.
- Zhong, S., Chai, H., Xu, Y., Li, Y., Ma, J.-Y., & Sun, W. (2017). Drought sensitivity of the carbon isotope composition of leaf dark-respired  $\text{CO}_2$  in  $\text{C}_3$  (*Leymus chinensis*) and  $\text{C}_4$  (*Chloris virgata* and *Hemarthria altissima*) grasses in Northeast China. *Frontiers in Plant Science*, 8, 1996.
- Zhu, B., & Cheng, W. (2011).  $^{13}\text{C}$  isotope fractionation during rhizosphere respiration of  $\text{C}_3$  and  $\text{C}_4$  plants. *Plant and Soil*, 342, 277–287.

## SUPPORTING INFORMATION

Additional supporting information may be found in the online version of the article at the publisher's website.

**How to cite this article:** McCloskey, C. S., Otten, W., Paterson, E., & Kirk, G. J. D. (2021). On allowing for transient variation in end-member  $\delta^{13}\text{C}$  values in partitioning soil C fluxes from net ecosystem respiration. *European Journal of Soil Science*, 72(6), 2343–2355. <https://doi.org/10.1111/ejss.13177>